Pertanika J. Sci. & Technol. 25 (4): 1211 - 1222 (2017)

SCIENCE & TECHNOLOGY

Journal homepage: http://www.pertanika.upm.edu.my/

# Analysis of PWM Techniques for Inverters Driving AC Motors

**Rajkamal R[1] and Anitha Karthi[2]***

*[1]Department of Electrical and Electronics Engineering, Madanapalle Institute of Technology and Science, Andhra Pradesh, India*
*[2]Department of Electrical and Electronics Engineering, Rajalakshmi Institute of Technology, Kuthambakkam, Chennai – 600 124, Tamil Nadu, India*

## ABSTRACT

Pulse Width Modulation (PWM) techniques are widely used in PV-operated, inverter-controlled AC motor drives. The frequency and magnitude of the voltage applied to the motors are controlled using PWM-based PV-operated drives. PWM is the standard approach for operating the inverter in order to generate high quality output voltage. In past decades, the performance of the PWM techniques were determined using power factor, transient response and efficiency, which play a major role in the regulation of PWM inverters so that a dynamic response can be obtained in grid-connected facilities. Conventional PWM such as PWM, Sinusoidal PWM (SPWM) and Space-Vector PWM (SVPWM) perform satisfactorily in terms of average switching frequency requirement, switching losses and DC bus current ripple, with respect to driving AC induction motors. However, they have poor harmonic characteristics leading to degradation of torque and speed profile of AC motor. In order to overcome the aforementioned drawback, the proposed work investigated the harmonic contents of the mentioned PWM techniques, torque and speed profiles with regards to the AC drive applications. The simulation study revealed that the 2nd, 5th and 8th order (negative sequence) harmonics introduced more problems related to torque and the 4th and 7th (positive sequence) harmonics created more heating problems. Further, the 3rd, 6th and 9th (zero sequence) harmonics caused heat due to addition of voltage and/or current in a neutral conductor. The main objective of the paper was to compare the three well established PWM methods with respect to the AC drive application in the context of effect of harmonics, by analysing their ease of implementation, output harmonic spectra voltage and Total Harmonic Distortion (THD).

*Keywords:* AC motor, pulse width modulation, speed, torque, total harmonic distortion

ARTICLE INFO

*Article history:*
Received: 08 May 2017
Accepted: 04 July 2017

*E-mail addresses:*
rajkamalr@gmail.com (Rajkamal R),
anithadkarthi@gmail.com (Anitha Karthi)
*Corresponding Author

ISSN: 0128-7680 

## INTRODUCTION

Inverters are classified into two types, voltage source and current source inverters. A voltage-fed inverter (VFI) or voltage-source inverter

(VSI) is one in which the DC source has small or negligible impedance and the input voltage is constant. A current-source inverter (CSI) is fed with adjustable current from the constant DC source of high impedance. A voltage source inverter employing thyristors as switches requires forced commutation, whereas VSIs using GTOs, power transistors, power MOSFETs or IGBTs can self-commutate by controlling base or gate drive signals.

Advances in solid-state power electronic devices, microprocessors and various inverter-control techniques employing pulse-width-modulation (PWM) are increasing in PV-operated AC motor drive applications. The frequency and magnitude of the voltage applied to the motors are controlled using PWM-based PV-operated drives. Power supplies used in older computers, other recent appliances and compact fluorescent light bulbs can cause changes in sine waves as shown in Figure 1a. Usage of capacitive power appliances causes brief disturbances. Battery chargers are examples of capacitive loads and the disturbance is shown in Figure 1b. A large power consumer can put more load on the power grid so that voltage drops, as shown in Figure 1c. Since inverters store electricity, they can be used to compensate for such disturbances (Industry Guide, 2013).

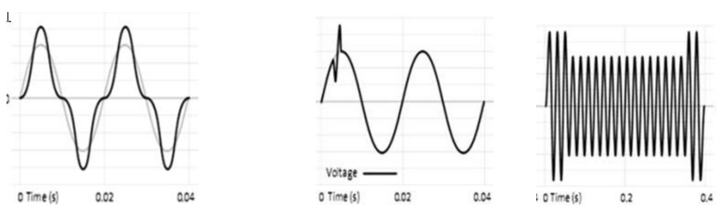


*Figure 1.* Possible disturbances due to (a). Fluorescent light load (b). Capacitive load (c). Overload (Industry Guide)

Implementation of a full bridge inverter, which is a single stage DC to AC conversion topology, is quite often used in PV inverters. Gonzalez (2007) proposed a topology that generates no common-mode voltage that exhibits high efficiency and can operate with any power factor. QuanLi (2008) implemented different topologies in a PV Module Integrated Converter (MIC) based on DC link configurations that provided a useful framework and point of reference for the next generationof MIC designs and applications. The increase in the number of pulses per half cycle, the order of dominant harmonic frequency can be raised and filtered out easily. Thus, an increase in switching frequency improves the quality of the output voltage waveform (Urmila Bandaru, 2011). PWM (Brundny, Szkudlapski, Morganti, & Lecointe, 2015) is the standard approach for operating an inverter in order to generate high quality output voltage. A PWM-based inverter is used to produce a controlled output current, which is in line with the utility voltage for obtaining a unity power factor (PF) for grid-connected facilities. In past decades, the performance of PWM techniques were determined using power factor, transient response and efficiency, which play a major role in the regulation of PWM inverters so that a dynamic response can be obtained in grid-connected facilities (Rong-Jong Wai, 2008). Conventional PWM such as PWM, Sinusoidal PWM (SPWM) and Space-Vector

PWM (SVPWM) perform satisfactorily in terms of average switching frequency requirement, switching losses and DC bus current ripple, with respect to driving AC induction motors (Leon, Kouro, Franquelo, Rodriguez, & Wu, 2016).

An AC chopper controller with symmetrical Pulse Width Modulation (PWM) achieves better performance for a single-phase induction motor compared to phase-angle control line-commutated voltage controllers and integral-cycle control of thyristors (Bashi, Mailah, & Cheng, 2008). The reduced switching frequency active-harmonic elimination method to eliminate any number of specific order harmonics using an FPGA controller is experimentally verified (Zhong Du, Tolbert, Chiasson, & Burak Ozpineci, 2008). Selective harmonic elimination pulse width modulation offers tight control of the harmonic spectrum of a given voltage and/or current waveform generated by a power electronic converter. Owing to its formulation and focus on elimination of low-order harmonics, it is highly beneficial for high-power converters operating with low switching frequencies (Mohamed, Konstantinou, & Agelidis, 2015).

Conventional PWM such as PWM, Sinusoidal PWM (SPWM) and Space-Vector PWM (SVPWM) perform satisfactorily in terms of average switching frequency requirement, switching losses and DC bus current ripple, with respect to driving AC induction motors (Hari, Pavan Kumar VSSS & Narayanan, G., 2016). However, they have poor harmonic characteristics leading to degradation of torque and speed profile of AC motor. Further, it is suggested that such poor harmonic characteristics can be improved by doing harmonics analysis followed by a suitable mitigation process. In Wai (2008), the harmonic contents of PWM techniques, torque and speed profiles were analysed based on the AC drive applications. The authors also designed an adaptive total sliding-mode control system for the current control of the PWM inverter to maintain the output current with a higher power factor and less variation under load changes. The above-mentioned PWM techniques are compared by analysing their ease of implementation, output harmonic spectra of output voltage and Total Harmonic Distortion (THD).

## ANALYSIS OF DISCONTINUOUS PWM

The output pulses are considered as a vector (with values of 0 or 1) depending on the operating mode (generator/motor) of the machine the output vector contains.

For the Arm 1 Bridge, two pulses are required: Pulse 1 is for the upper switch and Pulse 2 is for the lower switch.

For the Arm 2 Bridge, four pulses are required: Pulses 1 and 3 are, respectively, for the upper switches of the first and second arm. Pulses 2 and 4 are for the lower switches.

For the Arm 3 Bridge, six pulses are required: Pulses 1, 3 and 5 are, respectively, for the upper switches of the first, second and third arm. Pulses 2, 4 and 6 are for the lower switches.

For the double Arm 3 Bridges, twelve pulses are required: The first six pulses (Pulses 1 to 6) should be sent to the first Arm 3 bridge and the last six (Pulses 7 to 12) to the second Arm 3 bridge. Figure 2 shows the block diagram for discontinuous PWM generation.

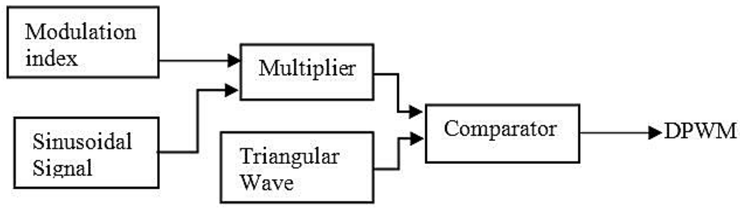


*Figure 2.* Block diagram – DPWM pulse generation

In this work control over frequency, modulation index and phase of the output voltage is obtained by internally-generated signals. The width of the input vector is 1 for single phase bridges (Arm 1 or Arm 2) and 3 for three-phase bridges (single or double bridge). In this work the three power switches are controlled by a switching signal *S*, while the remaining three switches are controlled inversely ($S^{-1}$).The switching signal is generated by the required voltage, $V_r$ and the triangle reference voltage, $V_D$. The switching frequency of the switches is constant and equals the frequency of the triangle voltage signal. The output voltage $V_0$ is either $V_{dcor}$ $-V_{dc}$. Figure 3a and Figure 3b show the stator voltage and current signals, respectively, obtained from the inverter based on DPWM.

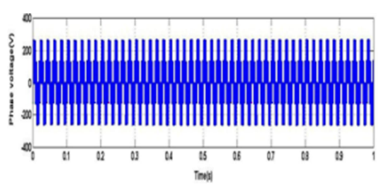

*Figure 3a.* Stator voltage – DPWM scheme

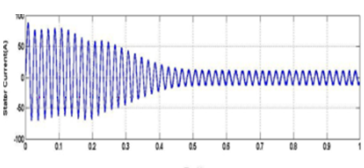

*Figure 3b.* Stator current – DPWM scheme

In-rush current or the starting current is free for any load attached; however, inertia and load of the motor have to be considered when the motor is connected to a load. The larger the inertia, the longer will be the time taken to reach full speed. As the motor accelerates, part of the starting current overcomes this inertia and is converted to kinetic energy. The remaining power of the starting current heats the rotor, up to possibly 250°C for a 'long' start (20 seconds). The current (I) is given by Equation [1] and Cos π is 0.3 during starting.

$$I = \frac{P(1.732 \times V)}{\cos \pi} \qquad [1]$$

where P=Power and V=Voltage.

Figure 4a and Figure 4b show the torque and speed characteristics of the motor when it is operated under the DPWM-based inverter. During the first couple of cycles of AC current, transient currents cause some of the phases to have higher asymmetrical values.

Torque (T) is represented by Equation [2].

$$T = \frac{sE_2^2 R_2}{R_2^2 + (sX_2)^2} \times \frac{3}{2\pi n_s} \qquad [2]$$

where s = Slip, $E_2$ = rotor voltage, $X_2$ = rotor reactance, $n_s$ = rotor speed in rps.

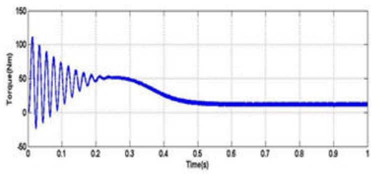


*Figure 4a.* Torque – DPWM scheme

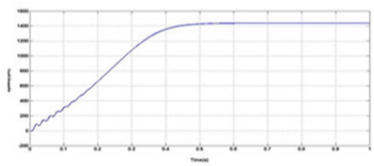

*Figure 4b.* Speed – DPWM scheme

It is also observed from Figure 4a and Figure 4b that the basic criteria of torque speed relation are satisfied as torque is inversely proportional to speed.

At s=1, the maximum starting torque occurs when rotor resistance equals rotor reactance. Total harmonics distortion analysis was carried out to find the harmonics present in voltage and the current applied to the machine when it is working under DPWM-based inverters. Figure 5a and Figure 5b show the THD values of harmonics content present in the voltage and current signals.

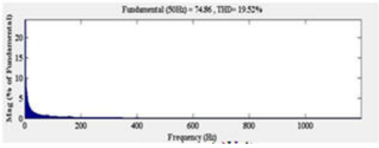


*Figure 5a.* THD in the voltage – DPWM scheme

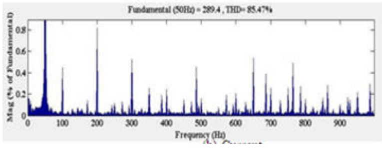


*Figure 5b.* THD in the current – DPWM scheme

## Analysis of Sinusoidal PWM

The Sinusoidal Pulse Width Modulation (SPWM) technique is the most popular technique for reduction of harmonics in inverters. The three sine waves are each displaced at an angle of 120° phase difference and are used for a three-phase inverter. The width of each pulse is varied in proportion to the amplitude of a sine wave evaluated at the centre of the pulse. It is achieved by comparing the desired reference waveform (modulating signal) with a high-frequency triangular wave. Depending on whether the signal voltage is larger or smaller than the carrier waveform, either the positive or negative DC bus voltage is applied at the output. Over the period of one triangle wave, the average voltage applied to the load is proportional to the amplitude of the signal during this period.

The SPWM technique uses constant amplitude pulses with different duty cycles. The pulse width is modulated to obtain inverter output voltage and helps to reduce its harmonic content.

In the SPWM technique three sine waves and a high frequency triangular carrier wave are used to generate a PWM signal.

Three reference sine waves each having an amplitude of 1V are generated with 00, 1200 and 2400 phase differences. The carrier triangular wave is generated by integrating the sine wave with a gain of 6500 and these reference signals are compared with carrier triangular waves of amplitude 1V, while the modulation index is kept as 1. To generate 32 kHz of switching frequency, a gain of 6500 is considered in this work (Muhammed H. Rashid, 2004). Switching pulses are generated whenever the width of the reference signal is greater than the carrier signal and these pulses trigger the switches.

The modulation process for generating pulses in SPWM is shown in Figure 6. The resulting wave is compared with the carrier signal using a relational operator, and it provides switching pulses for both the upper and lower switches.

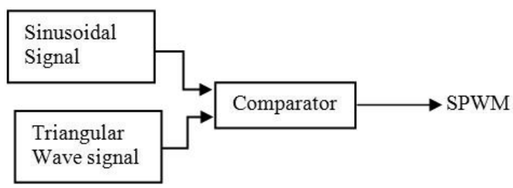


*Figure 6.* Block diagram – SPWM pulse generation

The unmodulated reference wave is again compared with the zero constant to eliminate negative halves and the result is multiplied with the total switching pulses to obtain the switching pulses for the upper switches and the inversion of the switching pulse of the upper switches is given to the switching pulse of the lower switches. The stator voltage, current, torque, speed and THD of the SPWM schema are obtained through simulation and shown in Figure 7a, Figure 7b, Figure 8a, Figure 8b, Figure 9a and Figure 9b, respectively.

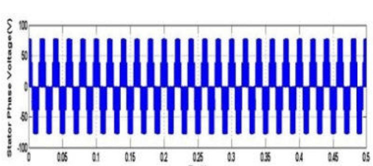

*Figure 7a.* Stator voltage – SPWM scheme

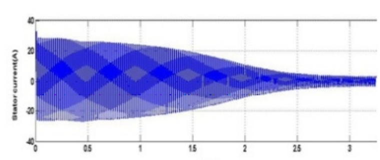

*Figure 7b.* Stator current – SPWM scheme

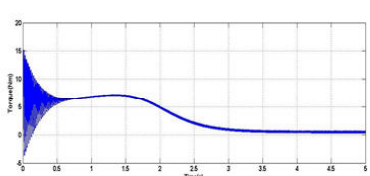

*Figure 8a.* Torque – SPWM scheme

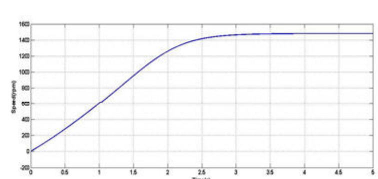

*Figure 8b.* Speed – SPWM scheme

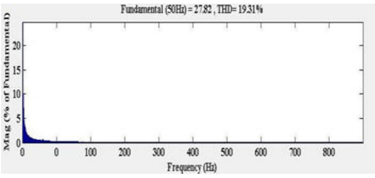


*Figure 9a.* THD in the voltage – SPWM scheme

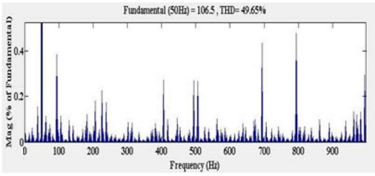


*Figure 9b.* THD in the current – SPWM scheme

## Analysis of Space Vector PWM

To implement the space vector PWM, the voltage equations in the abc reference frame is transformed into the stationary *d-q* reference frame that consists of the horizontal (d) and vertical (q) axes as shown in Figure 10 (Rait & Bhosale, 2011)

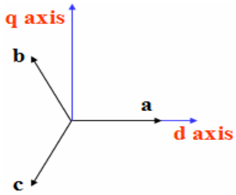


*Figure 10.* d-q frame

The output voltages of the inverter are composed of these eight switch states. Eight voltage vectors are defined, $U_0$= [000],$U_1$= [001], $U_2$= [010], $U_3$= [011], $U_4$= [100], $U_5$= [101], $U_6$= [110], $U_7$= [111] corresponding to the switch states $S_0$, $S_1$, $S_2$, $S_3$ $S_4$, $S_5$, $S_6$, $S_7$, respectively. The length of vectors $U_1$ to $U_6$ is unity and the length of $U_0$ and $U_7$ is zero and the form of these eight vectors are considered in the voltage-vector space.

$$\begin{aligned} &U_1 = -U_4 \\ &U_2 = -U_5 \\ &U_3 = -U_6 \\ &U_0 = U_7 = 0 \ \ and \\ &U_1 + U_3 + U_5 = 0 \end{aligned} \tag{3}$$

The voltage-vector space is divided into six sectors. In the vector space, according to the equivalence principle, the following operation rules are applied to satisfy the basic criteria of space-vector representation as shown in Figure 11.

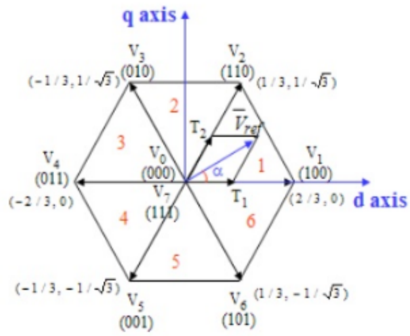


*Figure 11.* Space-Vector representation

The Pulse generation module of the SVPWM Scheme is shown in Figure 12.

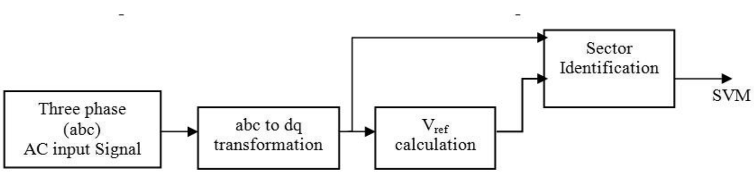


*Figure 12.* Block diagram – SVPWM pulse generation

The angle of the reference vector and switching time frame for each switch are determined by Equations [4], [5] and [6].

$$V_d = \frac{2}{3}(V_a \sin\omega t + V_b \sin(\omega t - 2\pi/3) + V_c \sin(\omega t + 2\pi/3)) \quad [4]$$

$$V_q = \frac{2}{3}(V_a \cos\omega t + V_b \cos(\omega t - 2\pi/3) + V_c \cos(\omega t + 2\pi/3)) \quad [5]$$

$$V_{ref} = V_d + jV_q \quad [6]$$

The magnitude and phase angle of Vref is obtained by

$$\left|V_{ref}\right| = \sqrt{V_d^2 + V_q^2} \quad [7]$$

$$\text{Angle} \quad \alpha = \tan^{-1}\left(\frac{V_d}{V_q}\right) \quad [8]$$

$$T_1 = \frac{\sqrt{3}T_z\left|V_{ref}\right|}{V_{dc}}\left(\sin\frac{n}{3}\pi\cos\alpha - \cos\frac{n}{3}\pi\sin\alpha\right) \quad [9]$$

$$T_2 = \frac{\sqrt{3}T_z\left|V_{ref}\right|}{V_{dc}}\left(\sin\alpha\cos\frac{n-1}{3}\pi - \cos\alpha\sin\frac{n-1}{3}\pi\right) \quad [10]$$

$$T_0 = T_z - T_1 - T_2 \qquad [11]$$

where n is the sector (1 to 6) and Tz is the switching time.

Like the previous schemes (DPWM, SPWM), stator voltage and current, torque and speed, voltage harmonics and current harmonics (IEEE Std 519-1992) are obtained through simulation as shown in Figure 13a, Figure 13b, Figure 14a, Figure 14b, Figure 15a and Figure 15b, respectively.

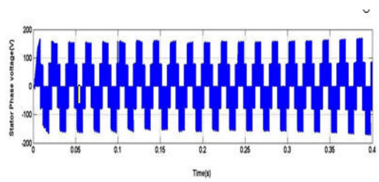

*Figure 13a.* Stator voltage – SVPWM scheme

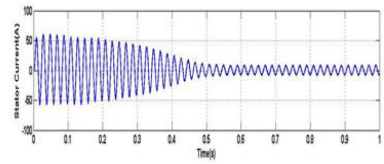

*Figure 13b.* Stator current – SVPWM scheme

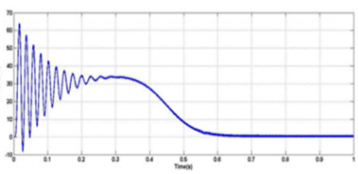

*Figure 14a.* Torque – SVPWM scheme

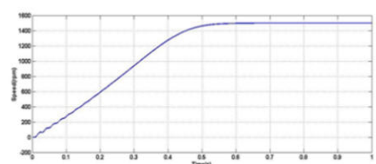

*Figure 14b.* Speed – SVPWM scheme

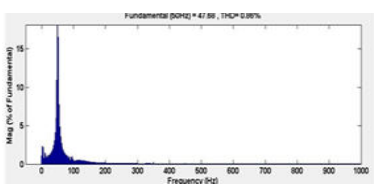

*Figure 15a.* THD in the voltage – SVPWM scheme

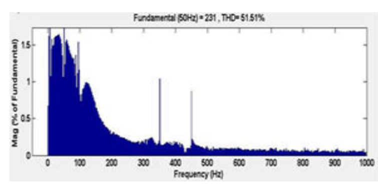

*Figure 15b.* THD in the current – SVPWM scheme

## Comparative Analysis

The simulation study of the DPWM, SPWM and SVPWM schemes are were obtained and the simulation results are shown from Figure 1 to 15. In this work, it was observed from Figures 4a, 8a and 14a that at low speeds, torque was not smooth. This led to disturbance of torque-slip characteristics. This effect was due to the current harmonics, particularly odd harmonics.

In Table 1, current and voltage harmonics are shown for all three schema. Further presence of even harmonics and odd harmonics with respect to fundamental frequency is shown in Table 2 and Table 3, respectively. From Table 1, 2 and 3 and from the simulation results it is evident that good torque i.e. speed profile for an AC drive application is maintained by the SVPWM, which allows less harmonics in output voltage and current signals.

Table 1
*Analysis of THD*

| THD | DPWM (%) | SPWM (%) | SVPWM (%) |
|---|---|---|---|
| Current Harmonics | 19.52 | 19.31 | 0.86 |
| Voltage Harmonics | 86.68 | 50.68 | 51.51 |

Table 2
*Analysis of Even Harmonics*

| Even Harmonics (% of fundamental) | | | |
|---|---|---|---|
| Order of harmonic | PWM | SPWM | SVPWM |
| 2 | 45 | 28 | 35 |
| 4 | 16 | 10 | 12 |
| 6 | 10 | 7 | 15 |
| 8 | 8 | 5 | 6 |
| 10 | 8 | 4 | 4.8 |

Table 3
*Analysis of Odd Harmonics*

| Odd Harmonics (% of fundamental) | | | |
|---|---|---|---|
| Order of harmonic | PWM | SPWM | SVPWM |
| 3 | 28 | 12 | 22 |
| 5 | 12 | 7.5 | 10 |
| 7 | 8 | 5.5 | 5.5 |
| 9 | 7.5 | 4.2 | 5.5 |
| 11 | 6 | 3.8 | 4 |

The comparative study showed that the SVPWM has advantages of lower harmonics and a higher modulation index compared with other PWM techniques. Because of its flexible manipulation of reference vector and modulation index, it is easy for complete digital implementation by a single chip microprocessor. Therefore, it is recommended that the SVPWM be used in motor control and power-converter applications. SVPWM is good with respect to minimum uncharacteristic harmonics compared with other modulation techniques such as conventional PWM and SPWM. However, each modulation technique is unique to the application for which it is employed.

## CONCLUSION AND FUTURE WORK

In this paper, the harmonic contents of the PWM, SPWM and SVPWM techniques, torque and speed profiles were investigated with regard to AC drive applications. The output harmonic spectra of output voltage and THD were analysed for the mentioned PWM techniques. A simulation study revealed that negative sequence harmonics introduced more problems related to torque and positive sequence harmonics created more heating problems. Further, zero sequence harmonics caused heat due to addition of voltage and/or current in a neutral conductor. From the simulation results, it was clear to see that the torque and speed profiles were completely unique for each modulation technique with respect to load (AC drives).

This work can be extended for all other types of load such as simple RLC and also all other industrial loads. This paper can be used as a guide for analysing the inverter in distributed energy resources that are integrated into the public power supply (grid) inputs. The various demands on inverters' effective operation are required for the grid as it requires sinusoidal alternating current (AC) with stable voltage and frequency and the harmonic component limits are regulated within the guidelines and standards. Modern inverters meet these power quality requirements, yet in some cases limits may be exceeded. Therefore, distributed generation is heavily dependent on the reliability and efficiency of the inverter.

## REFERENCES


Bandaru, U., & Rayudu, S. D. (2011). Harmonic orientation of pulse width modulation technique in multilevel inverters. *Advances in Electrical and Electronic Engineering, 9*(1), 29–34.

Bashi, S. M., Mailah, N. F., & Cheng, W. B. (2008). Development of a single-phase PWM AC controller. *Pertanika Journal of Science and Technology, 16*(2), 119–127.

Brudny, J. F., Szkudlapski, T., Morganti, F., & Lecointe, J. P. (2015). Method for controlling the PWM switching: Application to magnetic noise reduction. *IEEE Transactions on Industrial Electronics, 62*(1), 122-131.

Dahidah, M. S., Konstantinou, G., & Agelidis, V. G. (2015). A review of multilevel selective harmonic elimination PWM: formulations, solving algorithms, implementation and applications. *IEEE Transactions on Power Electronics, 30*(8), 4091-4106.

Du, Z., Tolbert, L. M., Chiasson, J. N., & Ozpineci, B. (2008). Reduced switching-frequency active harmonic elimination for multilevel converters. *IEEE Transactions on Industrial Electronics, 55*(4), 1761-1770.

F II, I. (1993). *IEEE recommended practices and requirements for harmonic control in electrical power systems.* New York, NY: IEEE.

Gonzalez, R, L. (2007). Transformer less inverter for single-phase photovoltaic systems. *IEEE Transactions on Power Electronics, 22*(2), 693-697.

Hari, V. P. K., & Narayanan, G. (2016). Space-vector-based hybrid PWM technique to reduce peak-to-peak torque ripple in induction motor drives. *IEEE Transactions on Industry Applications, 52*(2), 1489-1499.

Koenemann, D. D. (2013). *Inverter Storage and PV System Technology-Industry Guide 2013*. Solarpraxis AG, Berlin, Germany.

Leon, J. I., Kouro, S., Franquelo, L. G., Rodriguez, J., & Wu, B. (2016). The essential role and the continuous evolution of modulation techniques for voltage-source inverters in the past, present, and future power electronics. *IEEE Transactions on Industrial Electronics, 63*(5), 2688-2701.

QuanLi, W. (2008). *A review of the single phase photovoltaic module integrated converter topologies with three different DC link configurations* (pp. 1320–1333). IEEE Transactions on Power Electronics.

Rait, A. O., & Bhosale, P. (2011). FPGA Implementation of space vector PWM for speed control of 3-phase induction motor. *International Conference on Recent Advancements in Electrical, Electronics and Control* (pp. 221-225). Sivakasi, India.

Wai, R. J., & Wang, W. H. (2008). Grid-connected photovoltaic generation system. *IEEE Transactions on Circuits and Systems I: Regular Papers, 55*(3), 953-964.